Technical Research Report

Systems Research Center

Supported by the National Science Foundation Engineering Research Center Program (NSFD CD 8803012), the University of Maryland, Harvard University, and Industry

Analysis of Compressive Receivers for the Optimal Interception of Frequency-Hopped Waveforms

by W.E. Snelling and E. Geraniotis

TR 91-28

ANALYSIS OF COMPRESSIVE RECEIVERS FOR THE OPTIMAL INTERCEPTION OF FREQUENCY-HOPPED WAVEFORMS

William E. Snelling and Evaggelos Geraniotis

ANALYSIS OF COMPRESSIVE RECEIVERS FOR THE OPTIMAL INTERCEPTION OF FREQUENCY-HOPPED WAVEFORMS

William E. Snelling [1] and Evaggelos Geraniotis [2]

ABSTRACT

This paper establishes that the compressive receiver is a practical interceptor of high performance. Given a signal of a particular duration, a compressive receiver can estimate simultaneously all frequency components within a set wide band. This processing is similar to a parallel bank of narrowband filters, which is the optimal detector of frequency-hopped signals. Furthermore, hop frequency is estimated to yield performance equal to the parallel filter configuration. We assume interference to be stationary, colored Gaussian noise and present a model of the compressive receiver that contains all its salient features. Locally optimal detection is achieved by taking the compressive receiver output as an observation and applying likelihood ratio theory at small signal-to-noise ratios. For small signals, this approach guarantees the largest probability of correct detection for a given probability of false alarm and thus provides a reference, to which simplified or ad hoc schemes can be compared. Since the locally optimal detector has an unwieldy structure, a simplified suboptimal detector structure is developed that consists of simple filter followed by a sampler and a square-envelope detector. Several candidates for the filter's response are presented. The performance of the locally optimal detector based on compressive receiver observations is compared to the optimal filter-bank detector based on direct observations, thus showing the exact loss incurred when a compressive receiver is used. The performance of various simplified schemes based on compressive receiver observations is analyzed and compared with that of the locally optimal detector.

[1]Dr. W. E. Snelling is with The Johns Hopkins University Applied Physics Laboratory, Johns Hopkins Road, Laurel, MD 20723.

[2]Dr. E. Geraniotis is with the Department of Electrical Engineering and the Systems Research Center, University of Maryland, College Park, MD 20742.

This work was supported in part by the Systems Research Center at the University of Maryland, College Park, through the National Science Foundation's engineering Research Centers Program: NSF CDR 8803012

1. INTRODUCTION

The goal of the intercept receiver is to detect deceptive electromagnetic sources and extract waveform features for use in the exploitation or jamming of such sources. With the advent of frequency-hopped and other spread-spectrum signals, the search bandwidth that assures a reasonable probability of intercept has increased greatly, followed by a corresponding increase in the complexity of the intercept problem. Wideband interceptors are unacceptable and high-performing channelized interceptors virtually unimplementable. The compressive receiver, which simultaneously estimates frequency components over a set wide band, has promise as an interceptor with both the simplicity of a wideband device and the performance of the channelized device.

The literature contains a multitude of intercept methods for frequency-hopped waveforms (see [1], [2], [3], and [4]). There are also some analyses of the detection performance of the compressive receiver (see [5] and [6]). However, very little has been written on the application of the compressive receiver to the interception of spread-spectrum signals ([7] is an exception) and even less on the interception of frequency-hopped waveforms. Here we develop fully a locally optimal and a simplified suboptimal method for the detection of frequency-hopped waveforms.

We model the compressive-receiver input as consisting of either stationary Gaussian noise of known autocorrelation, or of noise plus a hopped signal of known hop epoch, unknown phase, and energy above a minimum detectable level. Approximate transfer relationships for signal and noise are developed separately and used to translate the detection problem to an equivalent one on the compressive-receiver output. Likelihood function theory is applied to the equivalent problem and yields a locally optimal detector (i.e. optimal for small signal-to-noise ratio). The locally optimal detector has an unwieldy structure that counters the leading motivation for using a compressive receiver: that of simplicity coupled with high performance. Therefore a suboptimal version, the simple-filter detector is developed that uses a time-invariant filter in place of the time-varying filter of the first. Asymptotic statistics of the detector's output are derived and used to quantify performance.

2. NOISE AND SIGNAL

Precise statistical models of the compressive-receiver input and of the receiver itself are in order. However, to statistically model the compressive receiver output we need transfer relationships for both the noise and the signal.

2.1. INPUT SIGNAL MODEL

Military and other secure communications use spread-spectrum signaling involving some variety of modulation, whose purpose is to add ambiguity or "randomness" to the waveform as a measure against unintended detection or interception. The usual procedure for randomizing the waveform is pseudo-random variation of transmission times (time hopping or TH), phases (direct sequence or DS), or frequencies (frequency hopping or FH). This paper concentrates solely on the interception of FH waveforms that have the form

$$s(t) = \sum_{i=1}^{N_h} x_i(t) \qquad (1)$$

where

$x_i(t)$ equals $\sqrt{2S'}\sin(\omega_{k_i}t + \theta_i)$ for $iT_h \leq t \leq (i+1)T_h$;

$\{\omega_k\}_{k=1}^{K}$ is a family of known frequencies within the spread-spectrum bandwidth;

$\{k_i\}$ are integer-valued, independent, uniformly distributed, random variables ranging inclusively between 1 and K;

$\{\theta_i\}$ are continuous, independent, uniformly distributed, random variables ranging between 0 and 2π that represent carrier phase;

S' is a real constant denoting the average signal energy;

T_h is a real constant denoting the epoch, or time duration, of each hop;

N_h is a positive integer denoting the number of hops during message transmission.

This general model of frequency-hopped waveforms includes a large number of modulations, such as frequency shift keying (FSK) and minimum shift keying (MSK). Some important modulations not included are those whose carrier phase is correlated from hop to hop as, for example, continuous phase FSK (CPFSK). Even for these cases, these results apply but may not be optimal.

The signal model is for a composite hypothesis problem. Specifically, given the observation $y(t)$, the problem is one of choosing between H_0, which is the hypothesis that an FH waveform is not present, and $H_{\gamma'}$, which is the hypothesis that an FH waveform is present with SNR γ' greater than some minimum SNR γ. The model is precisely

$$\begin{aligned} H_0: \quad y(t) &= n(t) \\ \text{versus} \qquad & \\ H_{\gamma'}: \quad y(t) &= s(t) + n(t) \qquad \gamma < \gamma' \end{aligned} \tag{2}$$

where the frequency-hopped waveform $s(t)$ is given by (1) and $n(t)$ is stationary colored Gaussian noise with variance σ_i^2 and autocorrelation function $\sigma_i^2 R_i(t)$. The hypothesized SNR γ' is related to the other model parameters by $\gamma' = S'T_h/\sigma_i^2$, while similarly the minimum SNR $\gamma = ST_h/\sigma_i^2$.

Significantly, the signal model allows for colored noise and is, therefore, quite general. Note that the model assumes that all signal parameters, except for amplitude and hop frequency, are known.

2.2 Receiver Model

Figure 1 blocks out the compressive-receiver model. The compressive receiver mixes the input signal $y_i(t)$ with a linearly frequency-modulated signal

$$\alpha(t) = \cos(\omega_0 t - \beta t^2) \qquad 0 \le t \le T_s \tag{3}$$

that scans downward in frequency from ω_0 to $\omega_0 - 2\beta T_s$. Here T_s is the scan time. The scanned waveform is input to a pulse compression filter, hence the name compressive receiver. The filter has impulse response

$$h(t) = \cos(\omega_0 t + \beta t^2)\, w(t) \qquad 0 \le t \le T_c \tag{4}$$

where $w(t)$ is a weighting function used to minimize energy spillover between signals of different frequencies. The output of the compressive receiver now follows as

$$y_o(t) = \int_0^{T_c} \alpha(t-\tau) y_i(t-\tau) h(\tau)\, d\tau \qquad T_c \le t \le T_s \tag{5}$$

$$= \quad x_o(t) + n_o(t) \tag{6}$$

where

$$x_o(t) \quad \triangleq \quad \int_0^{T_c} \alpha(t-\tau)x_i(t-\tau)h(\tau)\,d\tau \qquad T_c \le t \le T_s \tag{7}$$

$$n_o(t) \quad \triangleq \quad \int_0^{T_c} \alpha(t-\tau)n_i(t-\tau)h(\tau)\,d\tau \qquad T_c \le t \le T_s. \tag{8}$$

2.3. OUTPUT DUE TO SIGNAL

Using (3), (4), and the commuted version of (8) the output of the compressive receiver can be expressed as

$$x_o(t) = \int_{t-T_c}^{t} x(\tau)\cos(\omega_0\tau - \beta\tau^2)\cos\left[\omega_0(t-\tau) + \beta(t-\tau)^2\right] w(t-\tau)\,d\tau \tag{9}$$

whenever $T_c \le t \le T_s$. Trigonometric manipulation leads to

$$\begin{aligned} x_o(t) \quad = \quad & \frac{1}{2}\cos(\omega_0 t + \beta t^2)\int_{t-T_c}^{t} x(\tau)\cos(2\beta t\tau)w(t-\tau)\,d\tau \\ & + \frac{1}{2}\sin(\omega_0 t + \beta t^2)\int_{t-T_c}^{t} x(\tau)\sin(2\beta t\tau)w(t-\tau)\,d\tau + \epsilon. \end{aligned} \tag{10}$$

Application of Lemma 2 shows that

$$|\epsilon| \le \frac{P_w P_x}{\omega_0} \tag{11}$$

where P_w is the positive variation of the window $w(t)$ on $t \in [0, T_c]$ and where P_x is the positive variation of the input $x(t)$ on $t \in [0, T_s]$. The definition of positive variation appears as Definition 1 in Appendix B.

The error bound has special meaning when $X(t)$ is a sine wave of angular frequency ω. In this case, $P_x \approx \omega T_c/\pi \le 2\beta T_s T_c/\pi$ and hence

$$|\epsilon| \le 2\frac{P_w \beta T_s T_c}{\pi\omega_0} \tag{12}$$

which is very small for typical values of ω_0, T_c, T_s, and β.

2.4. OUTPUT DUE TO NOISE

As shown in Appendix A (84 and 88), the normalized autocorrelation (divided by σ_i^2) of the compressive-receiver output is

$$R_o(t,d) = \frac{1}{8}\int_{-T_c}^{T_c} R_i(u_1 - d)\Bigg\{ \int_{|u_1|}^{2T_c-|u_1|} \cos\left[(\omega_0 - 2\beta t + \beta u_2)(u_1 - d)\right]\cos\left[(\omega_0 + \beta u_2)u_1\right] w\left(\frac{u_2+u_1}{2}\right) w\left(\frac{u_2-u_1}{2}\right)\, du_2 \Bigg\}\, du_1 + \epsilon. \tag{13}$$

The error term ϵ is bounded as

$$|\epsilon| \leq \frac{1}{8}P_w^2 B T_c \tag{14}$$

where

$$B = \frac{1}{2\beta T_c} + \frac{1}{2\omega_0 - 2\beta T_s} + \frac{2}{\omega_0 - 2\beta T_s} + \frac{2}{\omega_0 - \beta T_c} \tag{15}$$

with P_w being the positive variation of $w(t)$ defined by Definition 1 in Appendix B.

Under typical operating constraints, the error bound can be simplified further. The term $2\beta(T_s - T_c)$ represents the total frequency spanned by the compressive filter, which is very large (typically on the order of megahertz). Additionally, the frequency ω_0 is usually in the tens to hundreds of megahertz range, hence $\omega_0 \gg 10^6$. These two facts, along with the fact that the scan time is typically twice the compression time (i.e. $T_s = 2T_c$), imply that $B < 1/\beta T_c$. Under these assumptions, the error is bounded as

$$|\epsilon| < \frac{1}{8}\frac{P_w^2}{\beta}. \tag{16}$$

Of interest are special cases of the autocorrelation. When the input noise is white, meaning[3] that $\sigma_i^2 R_i(t) = \delta(t)N_0/2$, then the output noise is stationary and has autocorrelation

$$R_o(d) = \frac{1}{16}\int_{|d|}^{2T_c-|d|} \cos\left[|d|(\omega_0 + \beta u_2)\right] w\left(\frac{u_2+|d|}{2}\right) w\left(\frac{u_2-|d|}{2}\right)\, du_2 \tag{17}$$

whenever $|d| \leq T_c$, otherwise $R_o(d) = 0$. If the window function w is rectangular, then

$$R_o(d) = \frac{1}{8}\,\frac{\sin\left[\beta|d|(T_c - |d|)\right]}{\beta|d|}\cos\left[|d|(\omega_0 + \beta T_c)\right] \tag{18}$$

[3]Since the variance of a white noise process is undefined, arbitrarily let $\sigma_i^2 = N_0$ where N_0 is the single-sided spectral density of the white noise process. This choice make the signal-to-noise ratio, γ, consistent with other definitions in the literature.

whenever $|d| \leq T_c$, otherwise $R_o(d) = 0$. Regressing to the case of general stationary noise but now considering only rectangular windows,

$$R_o(t,d) = \frac{1}{8}\int_{-T_c}^{T_c} R_i(u_1 - d) g(u_1, t, d)\, du_1 \tag{19}$$

where

$$\begin{aligned} g(u_1,t,d) = &\frac{\sin\left[(\beta d - 2\beta u_1)(T_c - |u_1|)\right]}{(\beta d - 2\beta u_1)} \\ &\times \cos\left[\omega_0 d + 2\beta t(u_1 - d) - 2\omega_0 u_1 + (\beta d - 2\beta u_1)T_c\right] \\ &+ \frac{\sin\left[\beta d(T_c - |u_1|)\right]}{\beta d}\cos\left[\omega_0 d + 2\beta t(u_1 - d) + \beta d T_c\right]. \end{aligned} \tag{20}$$

3. LOCALLY OPTIMAL DETECTOR

We aim at developing a locally optimal detector of frequency-hopped waveforms based on a compressive receiver output. Capitalizing on the fact that the optimal detector of frequency-hopped waveforms integrates coherently over a single hop period [4], we conjecture that an optimally configured compressive receiver should integrate over a period commensurate with the hop epoch T_h. But we also want to avoid interhop interference, thus we choose $T_s = T_h$ and assume that the compressive receiver is synchronized to frequency hops. This is not a realistic assumption in the pure detection problem but one that leads to an optimal detector, whose performance degrades gracefully upon relaxing this assumption.

Because the interfering noise is typically of much larger bandwidth than the hop rate, the correlation between hops is negligible and so the optimal multihop detection statistic is some kind of combination of single-hop detection statistics. We thus confine ourselves to the problem of using the compressive receiver to optimally detect, given an observation period of T_s, a sine wave of unknown amplitude and phase and whose frequency is one of the known hop frequencies.

Based on the above assumptions, the detection problem is now

$$\begin{aligned} &H_0: & x_i(t) &= n_i(t) \\ \text{versus} \quad & & & \\ &H_{\gamma'}: & x_i(t) &= \sqrt{2S}\sin(\omega_k t + \theta) + n_i(t) \end{aligned} \tag{21}$$

for $\gamma < \gamma'$ and $T_c \leq t \leq T_s$. The parameters θ, γ, γ', ω_k, and $n_i(t)$ are as defined in Section 2.1.

Using the results in Sections 2.3 and 2.4 the detection problem based on the output of the compressive receiver becomes

$$\begin{aligned} H_0 : \quad x_o(t) &= n_o(t) \\ \text{versus} \qquad & \\ H_{\gamma'} : \quad x_0(t) &= \sqrt{2S'}\cos\theta\, y_c(t,\omega_k) + \sqrt{2S'}\sin\theta\, y_s(t,\omega_k) + n_o(t) \end{aligned} \tag{22}$$

for $\gamma < \gamma'$ and $T_c \leq t \leq T_s$, where $n_o(t)$ is stationary, colored Gaussian noise with autocorrelation function $R_o(t)$ as defined by (13) and

$$\begin{aligned} y_c(t,\omega_k) &\triangleq \frac{1}{2}\cos(\omega_0 t + \beta t^2)\int_{t-T_c}^{t} \cos(\omega_k\tau)\cos(2\beta t\tau)w(t-\tau)\, d\tau \\ &+ \frac{1}{2}\sin(\omega_0 t + \beta t^2)\int_{t-T_c}^{t} \cos(\omega_k\tau)\sin(2\beta t\tau)w(t-\tau)\, d\tau . \end{aligned} \tag{23}$$

$$\begin{aligned} y_s(t,\omega_k) &\triangleq \frac{1}{2}\cos(\omega_0 t + \beta t^2)\int_{t-T_c}^{t} \sin(\omega_k\tau)\cos(2\beta t\tau)w(t-\tau)\, d\tau \\ &+ \frac{1}{2}\sin(\omega_0 t + \beta t^2)\int_{t-T_c}^{t} \sin(\omega_k\tau)\sin(2\beta t\tau)w(t-\tau)\, d\tau . \end{aligned} \tag{24}$$

From [8], the conditional log-likelihood function for this problem becomes

$$\begin{aligned} &\ln\Lambda[x_o(t)/\omega_k,\theta,\gamma] = \\ &\sqrt{\frac{2\gamma}{\sigma_i^2 T_h}}\cos\theta\int_{T_c}^{T_s} x_o(\tau)g_c(\tau,\omega_k)\, d\tau + \sqrt{\frac{2\gamma}{\sigma_i^2 T_h}}\sin\theta\int_{T_c}^{T_s} x_o(\tau)g_s(\tau,\omega_k)\, d\tau - \\ &2\frac{\gamma}{T_h}\int_{T_c}^{T_s}[\cos\theta\, y_c(\tau,\omega_k) + \sin\theta\, y_s(\tau,\omega_k)]\,[\cos\theta\, g_c(\tau,\omega_k) + \sin\theta\, g_s(\tau,\omega_k)]\; d\tau \end{aligned} \tag{25}$$

where the functions $g_c(t,\omega_k)$ and $g_s(t,\omega_k)$ are respectively defined by the integral equations

$$\int_{T_c}^{T_s} R_o\left[\frac{\tau+t}{2}, \tau - t\right] g_c(\tau,\omega_k)\, d\tau = y_c(t,\omega_k) \tag{26}$$

$$\int_{T_c}^{T_s} R_o\left[\frac{\tau+t}{2}, \tau - t\right] g_s(\tau,\omega_k)\, d\tau = y_s(t,\omega_k) \tag{27}$$

for $T_c \leq t \leq T_s$. Since we are interested in a locally optimal test (i.e. small γ), we neglect the last term of (25) and say

$$\ln \Lambda\left[x_o(t)/\omega_k, \theta, \gamma\right] \approx \sqrt{\frac{2\gamma}{\sigma_i^2 T_h}} \cos\theta \int_{T_c}^{T_s} x_o(\tau) g_c(\tau, \omega_k)\, d\tau + \sqrt{\frac{2\gamma}{\sigma_i^2 T_h}} \sin\theta \int_{T_c}^{T_s} x_o(\tau) g_s(\tau, \omega_k)\, d\tau. \tag{28}$$

Averaging this approximate likelihood ratio over θ and ω_k yields

$$\Lambda\left[x_o(t)/\gamma\right] = \sum_{k=1}^{K} I_0 \left[\sqrt{\frac{2\gamma}{\sigma_i^2 T_h}} \left| \int_{T_c}^{T_s} x_o(\tau) G_k(\tau) \right| \right] \tag{29}$$

where I_0 is the modified Bessel function of the first kind and zero order and the complex-valued function $G_k(t)$ is defined as

$$G_k(t) \triangleq g_c(t, \omega_k) + i\, g_s(t, \omega_k). \tag{30}$$

Consider again the small γ case and note that $I_0(x) \approx 1 + x^2/4$, for small x. Conjure (29) into a locally optimal statistic

$$\Gamma = \frac{1}{\sigma_i^2 T_h} \sum_{k=1}^{K} \left| \int_{T_c}^{T_s} x_o(\tau) G_k(\tau)\, d\tau \right|^2 \tag{31}$$

where the scale factor $1/\sigma_i^2 T_h$ is added for convenience in future analyses. Figure 2 blocks out (31). To complete the detector, Γ is compared against a threshold v, whose value determines the probability of false alarm P_F. (Section 5 shows the exact relationship between v and P_F.) The statistic γ being locally optimal will, for small signal-to-noise ratios, yield the greatest possible probability of detection; hence it is locally the most powerful test.

4. SIMPLE-FILTER DETECTORS

The locally optimal detector of the previous section efficiently detects frequency-hopping waveforms. As will be shown, it rivals the optimal detector that directly observes the original time waveform. Unfortunately, it also rivals the optimal detector in implementation complexity and thus undermines the attractive simplicity of the compressive receiver. In this section, we construct detectors that maintain the simplicity of implementation for a small performance cost.

The simple-filter detector is depicted in Figure 3. It consists of a complex filter, with impulse response $H(t)$, whose squared output is sampled at times

$$t = T_s + (k-1)\Delta T \qquad \text{for } k = 1, \cdots, K \tag{32}$$

then summed and scaled by $1/\sigma_i^2 T_h$ to produce the test statistic $\widehat{\Gamma}$. It is easily shown that

$$\widehat{\Gamma} = \frac{1}{\sigma_i^2 T_h} \sum_{k=1}^{K} \left| \int_{T_c}^{T_s} x_o(\tau) H\left[T_s + (k-1)\Delta T - \tau\right] \, d\tau \right|^2 \tag{33}$$

which by defining

$$\widehat{G_k}(t) \triangleq H\left[T_s - t + (k-1)\Delta T)\right] \qquad \text{for } T_c \leq t \leq T_s \tag{34}$$

yields the alternate expression

$$\widehat{\Gamma} = \frac{1}{\sigma_i^2 T_h} \sum_{k=1}^{K} \left| \int_{T_c}^{T_s} x_o(\tau) \widehat{G}_k(\tau) \, d\tau \right|^2 . \tag{35}$$

Rewriting the test statistic in this form, a form analogous to that of the locally optimal test statistic, allows us to develop a performance measure that applies to both detector types.

The above detector structure has two unknowns, the filter response $H(t)$ and the sampling time ΔT. The best choices for $H(t)$ and ΔT have not been determined but four candidate pairs are investigated. They are the time-multiplexed detector, the time-averaged detector, the time-typical detector, and the truncated detector.

4.1 TIME-MULTIPLEXED DETECTOR

The fact that the G_ks and the output of the compressive receiver are almost nonzero only around the times corresponding to a particular hop frequency suggests that all the branches of the locally optimal detector can be approximately reformed (or time-multiplexed) as the sampled output of a single filter.

The filter response of the time-multiplexed detector is constructed from the pseudo-signals $G_k(t)$ by the equation

$$H(t) = \sum_{j=1}^{K} G_j\left[T_s - t + (j-1)\Delta T\right]. \tag{36}$$

Note that above equation transforms (34) to

$$\widehat{G}_k(t) = \sum_{j=1}^{K} G_j\left[(j-k)\Delta T + t\right] \tag{37}$$

which, for $\Delta T \geq T_s - T_c$ implies $\widehat{G}_k(t) = G_k(t)$, since the G_js are zero outside the range $T_c \leq t \leq T_s$. Hence the time-multiplexed detector is equivalent to locally optimal detector for this choice of ΔT. In general, the duty cycle of the detector can be lowered by enlarging ΔT to get performance as close to that of the locally optimal detector as desired.

4.2 TIME-AVERAGED DETECTOR

Experience shows that, up to a phase factor, the G_ks are approximately time shifted versions of each other. This suggests a procedure for producing $H(t)$. First to correct for phase differences, normalize each G_k with the value of G_k corresponding in time to the kth hop frequency. Next average the normalized G_k. We assume here that the hop frequencies are equally spaced with spacing, in time, as $(\omega_2 - \omega_1)/2\beta$. This spacing corresponds to the shift between the G_ks and will also be the value chosen for ΔT.

Using the above we write the filter response for the time averaged detector as

$$H(t) = \frac{1}{N(t)} \sum_{j=1}^{K} \frac{G_j\left[T_s - t + \frac{\omega_j - \omega_1}{2\beta}\right]}{G_j\left(\frac{\omega}{2\beta}\right)} \tag{38}$$

where $K - N(t)$ corresponds to the number of G_ks in the sum, whose arguments are outside the interval $[T_c, T_s]$ and therefore to zero. The function $N(t)$ is given by

$$N(t) = \sum_{j=1}^{K} I_{[T_c,T_s]}\left[T_s - t + \frac{\omega_j - \omega_1}{2\beta}\right] \tag{39}$$

with $I_{[T_c,T_s]}$ being the characteristic function of the interval $[T_c, T_s]$.

4.3 TIME-TYPICAL DETECTOR

The above observation that the G_ks are approximately time shifted also inspires the time-typical detector. Instead of using an average of the G_ks, we use a "typical" G_k that has been time extended to prevent the resultant filter from omitting observations during its integration. Specifically, define

$H(t) = G_T(T_s - t + K\Delta T/2)$, where

$$\int_{T_c-T_1}^{T_s+T_1} R_o\left[\frac{\tau+t}{2}, \tau - t\right] G_T(\tau)\, d\tau = Y_{K/2}(t) \tag{40}$$

where

$$Y_k(t) = y_c(t,\omega_k) + i y_s(t,\omega_k) \tag{41}$$

and the extended time, $T_1 = (T_s - T_c)/2$. As shown above, $\Delta T = (\omega_2 - \omega_1)/2\beta$.

4.4 TRUNCATED DETECTOR

Here we choose again $\Delta T = (\omega_2 - \omega_1)/2\beta$ and define

$$H(t) = Y_1(T_s - t), \qquad \frac{\omega_1 - \omega_2}{4\beta} \leq T_s - t \leq \frac{\omega_1 + \omega_2}{4\beta}. \tag{42}$$

This corresponds to a detector that applies direct correlation, as opposed to a pseudo-correlation, in a time-truncated region about the hop frequency. It uses the fact that each function $Y_k(t)$ is a time shifted version of each other which allows it to use a representative function $Y_1(t)$ in the correlation. The time truncation prevents cross correlation between the $\widehat{G}_k$s.

5. DETECTOR PERFORMANCE ANALYSIS

In both the locally optimal detector and the simple-filter detector, the test statistic is the sum of squares of a large number of weakly correlated random variables. Namely, for the locally optimal detector,

$$\Gamma = \sum_{j=1}^{2K} \zeta_j^2 \tag{43}$$

where

$$\zeta_j \triangleq \frac{1}{\sqrt{\sigma_i^2 T_h}} \int_{T_c}^{T_s} x_o(\tau) h_j(\tau)\, d\tau \tag{44}$$

and where $h_j(t)$ is defined as

$$h_{2m-1}(t) = g_c(t,\omega_m) \tag{45}$$

$$h_{2m}(t) = g_s(t,\omega_m) \tag{46}$$

with $1 \leq m \leq K$. Similarly, for the simple-filter detector, the test is

$$\hat{\Gamma} = \sum_{j=1}^{2K} \hat{\zeta}_j^2 \tag{47}$$

where

$$\hat{\zeta}_j \triangleq \frac{1}{\sqrt{\sigma_i^2 T_h}} \int_{T_c}^{T_s} x_o(\tau)\widehat{h}_j(\tau)\, d\tau \tag{48}$$

and, for $1 \leq m \leq K$,

$$\widehat{h}_{2m-1}(t) \triangleq \widehat{g}_c(t, \omega_m) \tag{49}$$

$$\widehat{h}_{2m}(t) \triangleq \widehat{g}_s(t, \omega_m). \tag{50}$$

Here, $\widehat{g}_c(t,\omega_m) \triangleq \Re\left[\widehat{G}_m(t)\right]$ and $\widehat{g}_s(t,\omega_m) \triangleq \Im\left[\widehat{G}_m(t)\right]$. In the analysis to follow, the hat notation will be dropped, since the results apply to each detector in the same way. In other words, to get the result for the simple-filter detector, add hats to the appropriate variables.

Because the test statistic is the sum of a large number of weakly correlated random variables, there is reason to believe, despite the correlation, that the statistic has approximately Gaussian distribution. We proceed under this assumption, which we justify later. To specify the asymptotic distribution of Γ, we need its mean and variance under the signal-present and signal-absent hypotheses. For this purpose, define $z_j(t)$, for $1 \leq j \leq 2K$, as

$$z_{2m-1}(t) = y_c(t, \omega_m) \tag{51}$$

$$z_{2m}(t) = y_s(t, \omega_m) \tag{52}$$

with m ranging between 1 and K, while $\bar{z}_j(t)$, for $1 \leq j \leq 2K$, is defined as

$$\bar{z}_{2m-1}(t) = \int_{T_c}^{T_s} R_o\left[\frac{t+\tau}{2}, t-\tau\right] g_c(\tau, \omega_m)\, d\tau \tag{53}$$

$$\bar{z}_{2m}(t) = \int_{T_c}^{T_s} R_o\left[\frac{t+\tau}{2}, t-\tau\right] g_s(\tau, \omega_m)\, d\tau \tag{54}$$

with m also ranging between 1 and K. For the same reason as above, we define the time cross-correlations

$$\xi_{m,n} = \frac{1}{T_h} \int_{T_c}^{T_s} z_m(\tau) h_n(\tau)\, d\tau \tag{55}$$

$$\bar{\xi}_{m,n} = \frac{1}{T_h} \int_{T_c}^{T_s} \bar{z}_m(\tau) h_n(\tau)\, d\tau \tag{56}$$

for $1 \le m, n \le K$. (For the locally optimal detector case, note that $\bar{\xi}_{j,k} = \xi_{j,k}$.) Assume now that the signal is at frequency ω_l. Then

$$\zeta_k = \sqrt{2\gamma'}\cos\theta\,\xi_{2l-1,k} + \sqrt{2\gamma'}\sin\theta\,\xi_{2l,k} + \eta_k \tag{57}$$

where the random variable θ is uniformly distributed on $[0, 2\pi]$ and the η_ks are zero-mean Gaussian with covariances $\mathcal{E}(\eta_j\eta_k) = \bar{\xi}_{j,k}$. From (121) in Appendix C,

$$\mu_{k/l} \triangleq \mathcal{E}(\zeta_k^2/\omega_l) = \gamma'(\xi_{2l-1,k}^2 + \xi_{2l,k}^2) + \bar{\xi}_{k,k}. \tag{58}$$

When averaged over l and summed over k, the mean of Γ is

$$M_{\gamma'} = \frac{\gamma'}{K}\sum_{k=1}^{2K}\sum_{l=1}^{2K}\xi_{k,l}^2 + \sum_{k=1}^{2K}\bar{\xi}_{k,k}. \tag{59}$$

Use (57) and (125) to construct the covariance between the jth and kth terms of Γ, when the signal is at frequency ω_l. The result is

$$\begin{aligned}\nu_{j,k/l} \;=\;& 2(\gamma')^2\,\xi_{2l-1,j}\,\xi_{2l,j}\,\xi_{2l-1,k}\,\xi_{2l,k} + \frac{(\gamma')^2}{2}\,\xi_{2l-1,j}^2\,\xi_{2l-1,k}^2 + \frac{(\gamma')^2}{2}\,\xi_{2l,j}^2\,\xi_{2l,k}^2 \\ -\;& \frac{(\gamma')^2}{2}\,\xi_{2l-1,j}^2\,\xi_{2l,k}^2 - \frac{(\gamma')^2}{2}\,\xi_{2l,j}^2\,\xi_{2l-1,k}^2 + 4\gamma'\xi_{2l-1,j}\xi_{2l-1,k}\bar{\xi}_{j,k} \\ +\;& 4\gamma'\xi_{2l,j}\xi_{2l,k}\bar{\xi}_{j,k} + 2\,\bar{\xi}_{j,k}^2\end{aligned} \tag{60}$$

which, upon averaging over l and summing over j and k, becomes

$$\begin{aligned}V_{\gamma'} =&\\ &\frac{(\gamma')^2}{K}\sum_{j=1}^{2K}\sum_{k=1}^{2K}\sum_{l=1}^{K}\left(2\,\xi_{2l-1,j}\,\xi_{2l,j}\,\xi_{2l-1,k}\,\xi_{2l,k} - \frac{1}{2}\,\xi_{2l-1,j}^2\,\xi_{2l,k}^2 - \frac{1}{2}\,\xi_{2l,j}^2\,\xi_{2l-1,k}^2\right) \\ +\;& \frac{\gamma'}{K}\sum_{j=1}^{2K}\sum_{k=1}^{2K}\sum_{l=1}^{2K}\left(\frac{\gamma'}{2}\,\xi_{l,j}^2\,\xi_{l,k}^2 + 4\,\xi_{l,j}\,\xi_{l,k}\,\bar{\xi}_{j,k}\right) + 2\sum_{j=1}^{2K}\sum_{k=1}^{2K}\bar{\xi}_{j,k}^2.\end{aligned} \tag{61}$$

Of course, for the signal-not-present case, the mean and variance are simply (59) and (61) with the signal-to-noise ratio $\gamma' = 0$.

Since the test statistic Γ has an approximately Gaussian distribution, the threshold υ and probability of detection P_D for a given probability of false alarm are

$$\upsilon = \sqrt{V_0}\,\Phi^{-1}(1 - P_F) + M_0 \tag{62}$$

and

$$P_F = 1 - \Phi\left(\frac{\sqrt{V_0}\Phi^{-1}(1-P_F) - M_{\gamma'} + M_0}{\sqrt{V_{\gamma'}}}\right) \tag{63}$$

where $\Phi(x)$ is the distribution function of the standard Gaussian.

Now we justify the use of the Central Limit Theorem (CLT). First let

$$\boldsymbol{\Sigma} \triangleq \begin{bmatrix} \bar{\xi}_{1,1} & \cdots & \bar{\xi}_{1,2K} \\ \vdots & & \vdots \\ \bar{\xi}_{2K,1} & \cdots & \bar{\xi}_{2K,2K} \end{bmatrix} \tag{64}$$

which is the covariance matrix of the ζ_is, and

$$\boldsymbol{E}_{\theta,l} \triangleq \begin{bmatrix} \xi_{2l-1,1}\cos\theta + \xi_{2l,1}\sin\theta \\ \vdots \\ \xi_{2l-1,2K}\cos\theta + \xi_{2l,2K}\sin\theta \end{bmatrix} \tag{65}$$

which are $1/\sqrt{2\gamma'}$ times the means of the ζ_is, under the condition that the signal has phase θ and frequency ω_l. We note that, since $\boldsymbol{\Sigma}$ is nonnegative definite and symmetric, there exists a square-root matrix $\boldsymbol{\Sigma}^{\frac{1}{2}}$ such that $\boldsymbol{\Sigma}^{\frac{T}{2}}\boldsymbol{\Sigma}^{\frac{1}{2}} = \boldsymbol{\Sigma}$. Consider also the diagonalization of $\boldsymbol{\Sigma} = \boldsymbol{T}^T\boldsymbol{\Lambda}\boldsymbol{T}$ where

$$\boldsymbol{\Lambda} = \begin{bmatrix} \lambda_1 & 0 & \cdots & 0 \\ 0 & \lambda_2 & \cdots & 0 \\ \vdots & \vdots & \vdots & \vdots \\ 0 & 0 & \cdots & \lambda_{2K} \end{bmatrix} \tag{66}$$

is the matrix of eigenvalues of $\boldsymbol{\Sigma}$ and $\boldsymbol{T}$ is an orthogonal matrix of eigenvectors. We use the above diagonalization and $\boldsymbol{\Sigma}^{\frac{1}{2}}$ to rewrite the test statistic as

$$\Gamma = \left(\boldsymbol{G} + \sqrt{2\gamma'}\boldsymbol{M}_{\theta,l}\right)^T \boldsymbol{\Lambda}\left(\boldsymbol{G} + \sqrt{2\gamma'}\boldsymbol{M}_{\theta,l}\right) \tag{67}$$

where

$$\boldsymbol{G} = \begin{bmatrix} g_1 \\ \vdots \\ g_2 \end{bmatrix} \tag{68}$$

with $\{g_i\}$ independent, zero mean, unity variance, and Gaussian and where

$$M_{\theta,l} \triangleq \begin{bmatrix} m_{1,\theta,l} \\ \vdots \\ m_{n,\theta,l} \end{bmatrix} = T^T \Sigma^{-\frac{1}{2}} E_{\theta,l}. \tag{69}$$

The test statistic Γ is now the sum of squares of independent Gaussian variables. Through application of the Berry-Esseén Theorem (see [9]), Γ conditioned on θ and l is approximately Gaussian distributed with an error no more than $4c/\sigma$, where

$$c = \max_{i,\theta,l} \lambda_i \frac{48\gamma' m_{i,\theta,l}^2 + 7}{8\gamma' m_{i,\theta,l}^2 + 2} \tag{70}$$

$$\sigma^2 = \sum_{i=1}^{2K} \lambda_i^2 (8\gamma' m_{i,\theta,l}^2 + 2). \tag{71}$$

If this error bound is small (a fact that must be established numerically) then the CLT applies uniformly to the conditional distribution of Γ. If, in addition, the overall mean $M_{\gamma'}$ and variance $V_{\gamma'}$ remain essentially constant with respect to l and θ, then the CLT applies to the unconditional distribution of Γ as well. This fact must be also established numerically.

The above analysis using the asymptotic distribution of Γ is supplemented with upper- and lower-bounding distributions. Specifically,

$$1 - Q_K \left[\sqrt{2\gamma' e_{\max}}, \sqrt{\frac{a}{\lambda_{\max}}} \right] \leq \Pr[\Gamma \leq a] \leq 1 - Q_K \left[\sqrt{2\gamma' e_{\min}}, \sqrt{\frac{a}{\lambda_{\min}}} \right] \tag{72}$$

where $\lambda_{\max}$, $\lambda_{\min}$ are respectively the maximum and minimum eigenvalues of the covariance Σ and where $e_{\max}$, $e_{\min}$ are respectively the maximum and minimum over all eigenvalues of the matrices

$$B_l \triangleq A_l^T \Sigma A_l, \quad 1 \leq l \leq K \tag{73}$$

with

$$A_l \triangleq \begin{bmatrix} \xi_{2l-1,1} & \xi_{2l,1} \\ \vdots & \vdots \\ \xi_{2l-1,2K} & \xi_{2l,2K} \end{bmatrix} \tag{74}$$

and, finally, where Q_m is the generalized Marcum Q-function defined as

$$Q_m(\alpha, \beta) \triangleq \int_\beta^\infty x \left(\frac{x}{\alpha}\right)^{m-1} e^{-\frac{1}{2}(x^2+\alpha^2)} I_{m-1}(\alpha x)\, dx. \tag{75}$$

Of interest is that the upper bound equals the lower bound only when the channel outputs are statistically independent and the sum of the square magnitude of the signal component across the channels is independent of signal phase. In a sense, the bounds give an indication of how well the detector fits the independent channel assumption, since the upper bound corresponds to the detector distribution under the channel and phase independence assumptions, but with an increased noise level, while the lower bound has the same interpretation, but with a decreased noise level. These bounds, when averaged, approximate the detector distribution, the usefulness of which will be studied and compared with the asymptotic distribution in the next section.

6. PERFORMANCE COMPARISONS

This section graphically compares the performance of the locally optimal detector based on the compressive-receiver output, to that of the optimal detector based on receiver input. Also evaluated is the performance of the simple-filter detector with various filter responses defined above.

Because the interceptor typically receives signals from the sidelobes of the emitter, it must observe several hops before a reliable detection can be made. Therefore, the detector described above has been extended to multiple hops (as was done in [4]). The parameters chosen for making comparisons are the following: $T_c = 50\ \mu s$, $T_s = 100\ \mu s$, $\omega_0 = 2\pi \times 40$ Mhz; the 100 hop frequencies are evenly distributed between 2.33 Mhz and 4.33 Mhz; the hop rate is 10 Khops/sec; and the detectors use a 1000 hop observation. The chosen noise is bandpass between 2 and 4 Mhz with uniform spectral density $N_0/2$.

Bandpass noise, uniformly distributed over the analysis band of the compressive receiver, produces noise on the output of the compressive receiver that has autocorrelation corresponding very closely to that due to white noise but reduced by a factor of two. This accounts for the accurate use of one half of (18) throughout the literature for compressive receiver performance evaluations, even though their model assumes white noise interference. We also use this approximation, which is realistic because, if the noise was truly white, it could be filtered into bandpass noise without loss of signal information; moreover, it can be shown numerically that one half of (18) corresponds to the true autocorrelation, given by (19), to within .1 % for the parameters chosen here.

Figure 4 shows how the locally optimal detector based on compressive receiver observations compares with the optimal, filter-bank detector based on direct observations. The plot consists of probability of detection curves over the SNR range -10 to 0 dB and for the probability of false alarms; .1, .01, .001. As expected, for low SNRs, the locally optimal and the optimal compare favorably. On the other hand, there is about a 1 dB difference between the performances in the 0 dB SNR region. Two factors are responsible. One is that the compressive receiver detector integrates only half as much data for each spectrum estimate as the filter-bank detector. At first, this suggests there should be about a 3 dB performance difference but because the compressive receiver detector observes a span of spectrum estimates, it indirectly uses more of the raw observations. The second reason behind the performance difference is that the optimal, filter-bank detector used here was constructed to be most powerful at 0 dB and hence performs better than any other detector at this SNR, but, if one considers average performance over a range of SNRs, then the discrepancies between the two detectors lessen.

Figure 4 also compares the two analyses of the locally optimal, compressive receiver detector. We conclude from the figure that the CLT analysis is optimistic by an amount that increases with the false-alarm probability and with SNR. It is even optimistic to the point of producing detection probability estimates above those of the upper- and lower-bounding distributions. The dependence on the false alarm probability is due to inaccurate estimation of the tail of the density representing the compressive receiver output. The detector output, being the sum of squares, must be positive but the asymptotic density introduced by the CLT allows a false, nonzero probability for negative detector output. Hence, the false alarm probability will be overestimated causing an unduly low detector threshold and corresponding optimistic detection probability. The dependence on the SNR stems from the fact that the CLT poorly models the detector output when one channel dominates, as in the high SNR case. Even though the optimistic estimate produced by the CLT analysis is above the upper and lower bounds, it is still useful because of its simplicity and because it provides a comparison with the filter-bank detector, which was analyzed via the CLT and hence is similarly optimistic.

Figure 5 compares the performance between the locally optimum, compressive-receiver detector and the simple-filter, compressive-receiver detector with each of the four filter responses described above (time multiplexed, time averaged, time typical, and truncated). Again the plot consists of probability of detection curves over the SNR range, -10 to 0 db, and for the probability of false alarms .1, .01, .001. The sampling time for the simple-filter detector is $\Delta T = (T_s - T_c)/4$, for the time-multiplex response, and $\Delta T = (\omega_2 - \omega_1)/2\beta$, for the other cases. The figure clearly shows the superiority of the truncated filter response, whose performance is degraded by only 3 dB over the locally optimum detector at 0 dB SNR. Interestingly, the truncated filter response makes no use of the whitening G_ks of the locally optimum detector and yet has superior performance over the other responses that do. Presumably this phenomenon is due to the fact that the G_ks perform a deconvolution and hence are unstable due to the perturbations that have transformed them into the simple-filter response. Since the truncated filter response makes no use of the noise correlation, producing a filter response directly from some optimality consideration may indeed produce a detector with performance closer to the locally optimal.

8. CONCLUSIONS

Presented in this paper are two detectors of frequency-hopped waveforms based on the compressive receiver. The first, the locally optimum detector, was developed by applying the likelihood-ratio theory to the observed compressive-receiver output and yielded a locally optimal (low-SNR) detector. The second, the simple-filter detector, was a simplified version that used a time-invariant filter in place of the time-varying filter of the first. Performance of both detectors were analyzed and compared.

The compressive receiver fulfills its promise as a simple, yet high-performing interceptor. The performance of the locally optimal detector shows that relatively little detectability is lost in the compressive receiver processing (no more than 1 dB for the SNR range investigated). Most of the discrepancy is due to the difference in coherent integration time (one-half for the parameters used). Because of its complexity, the locally optimum detector is only useful as an upper performance bound but, for a small performance cost (no more than 3 dB for the SNR range investigated), the simplicity of the compressive-receiver approach is retained by the simple-filter detector. It is very likely that a filter response exists that recaptures some this performance loss but that possibility was not pursued here.

APPENDIX A

Derivation of Compressive-Receiver Autocorrelation

The normalized autocorrelation of the compressive receiver output is defined to be

$$R_o(t,d) = \frac{1}{\sigma_i^2} E\left[n_o\left(t+\frac{d}{2}\right) n_o\left(t-\frac{d}{2}\right)\right] \tag{76}$$

under the restrictions that

$$T_c \le t \le T_s \tag{77}$$

and

$$\frac{|d|}{2} \le \min(t - T_c,\ T_s - t). \tag{78}$$

Substitute the expression for the output noise (8), interchange expectations and integration, and use the definition of the normalized input correlation $R_i(\tau) = \mathcal{E}[n_i(t)n_i(t+\tau)]/\sigma_i^2$ to get

$$\begin{aligned}
R_o(t,d) = \\
&\frac{1}{\sigma_i^2}\int_0^{T_c}\int_0^{T_c} R_i(\tau_1-\tau_2-d) \\
&\cos\left[\omega_0\left(t+\frac{d}{2}-\tau_1\right)-\beta\left(t+\frac{d}{2}-\tau_1\right)^2\right]\cos\left[\omega_0\tau_1+\beta\tau_1^2\right]w(\tau_1) \\
&\cos\left[\omega_0\left(t-\frac{d}{2}-\tau_2\right)-\beta\left(t-\frac{d}{2}-\tau_2\right)^2\right]\cos\left[\omega_0\tau_2+\beta\tau_2^2\right]w(\tau_2)\,d\tau_2\,d\tau_1.
\end{aligned} \tag{79}$$

To exploit the stationarity of the input noise, first transform the above integral with

$$u_1 = \tau_1 - \tau_2 \tag{80}$$

$$u_2 = \tau_1 + \tau_2 \tag{81}$$

and then reduce the cosine components with multiple applications of the identity

$$\cos(A)\cos(B) = 1/2\cos(A+B) + 1/2\cos(A-B) \tag{82}$$

to form

$$R_o(t,d) = \frac{1}{16}\int_{-T_c}^{T_c} R_i(u_1-d)\sum_{j=1}^{8}\Big\{$$

$$\int_{|u_1|}^{2T_c-|u_1|} \cos(\theta_j + \omega_j u_2 + \beta_j u_2^2) w\left(\frac{u_2+u_1}{2}\right) w\left(\frac{u_2-u_1}{2}\right) du_2 \Bigg\} du_1 \tag{83}$$

where θ_j, ω_j, and β_j are given by Table 1. Use more trigonometry and apply Lemma 2 to terms 3–8 to rewrite the autocorrelation as

$$\begin{aligned} R_o(t,d) =& \frac{1}{8}\int_{-T_c}^{T_c} R_i(u_1 - d)\Bigg\{ \\ & \int_{|u_1|}^{2T_c-|u_1|} \cos\left[(\omega_0 - 2\beta t + \beta u_2)(u_1 - d)\right]\cos\left[(\omega_0 + \beta u_2)u_1\right] \\ & w\left(\frac{u_2+u_1}{2}\right) w\left(\frac{u_2-u_1}{2}\right) du_2 \Bigg\} du_1 + \epsilon \end{aligned} \tag{84}$$

with error term

$$|\epsilon| \leq \frac{1}{8}P_w^2 \sum_{j=1}^{6} \int_{-T_c}^{T_c} \frac{|R_i(u_1-d)|}{(\omega_j + 2\beta_j|u_1|)}\, du_1 \tag{85}$$

where P_w^2 is the positive variation of $w(t)$ defined by Definition 1 of Appendix B. Simplify the error bound by minimizing each term $\omega_j + 2\beta_j|u_1|$ with respect to u_1, d, and t, while noting the restrictions (77) and (78). The result is

$$|\epsilon| \leq \frac{1}{8}P_w^2 B \int_{-T_c}^{T_c} |R_i(u_1 - d)|\, du_1 \tag{86}$$

where

$$B = \frac{1}{2\beta T_c} + \frac{1}{2\omega_0 - 2\beta T_s} + \frac{2}{\omega_0 - 2\beta T_s} + \frac{2}{\omega_0 - \beta T_c}. \tag{87}$$

The relation $|R(t)| \leq 1$ further simplifies the bound as

$$|\epsilon| \leq \frac{1}{8}P_w^2 B T_c. \tag{88}$$

APPENDIX B

Bounds on Integrals of Linearly Frequency-Modulated Sinusoids

The first bound (Lemma 1) is a tool used only to prove the second bound (Lemma 2) which is used for derivations concerning the output of the compressive receiver: namely, the derivation of the noise autocorrelation and the derivation of a simplified expression for the output signal component.

Lemma 1 *Under the restrictions that* $b > a$, $\omega > 0$, $\beta \geq 0$, *and* $\omega + 2\beta a > 0$,

$$\left| \int_a^b \cos(\theta + \omega t + \beta t^2)\, dt \right| \leq \frac{2}{\omega + 2\beta a}. \tag{89}$$

Proof

Define the function

$$\Upsilon(\theta, \omega, \beta) = \int_0^{t_\pi} \sin(\tilde{\theta} + \omega t + \beta t^2)\, dt \tag{90}$$

where

$$t_\pi = \begin{cases} \dfrac{-1 + \sqrt{1 + 4\beta(\pi - \tilde{\theta})}}{2\beta} & \beta > 0 \\ \dfrac{\pi - \tilde{\theta}}{\omega} & \beta = 0 \end{cases} \tag{91}$$

$$\tilde{\theta} = \theta \bmod \pi. \tag{92}$$

This is simply the integral of $\sin(\tilde{\theta} + \omega t + \beta t^2)$ from $t = 0$ to its first zero crossing.

Preliminarily, three facts need to be proven: first, that $\Upsilon(\theta, \omega, \beta)$ decreases with respect to β; second, that it decreases with respect to ω; and third, that with $\beta = 0$ it decreases with respect to $\tilde{\theta}$.

Beginning with the first fact we will show that $\Upsilon(\theta, \omega, \beta)$ decreases with respect to β by proving its partial derivative to be negative. Employ the chain rule to get

$$\frac{\delta \Upsilon(\theta, \omega, \beta)}{\delta \beta} = \int_0^{t_\pi} t^2 \cos(\tilde{\theta} + \omega t + \beta t^2)\, dt. \tag{93}$$

Let $x = t/t_\pi$ and observe that $\beta t_\pi^2 = \pi - \tilde{\theta} - \omega t_\pi$; then

$$\frac{\delta \Upsilon(\theta, \omega, \beta)}{d\beta} = t_\pi^3 \int_0^1 x^2 \cos[\tilde{\theta} + \omega t_\pi x + (\pi - \tilde{\theta} - \omega t_\pi) x^2]\, dx. \tag{94}$$

To tightly bound the above integral, find its supremum by observing that from $\omega t_\pi > 0$ follows $\tilde{\theta} + \omega t_\pi x + (\pi - \tilde{\theta} - \omega t_\pi) x^2 > \pi x^2$ on $x \in [0, 1]$, from which

$$\int_0^1 x^2 \cos\left[\tilde{\theta} + \omega t_\pi x + (\pi - \tilde{\theta} - \omega t_\pi) x^2\right]\, dx < \int_0^1 x^2 \cos(\pi x^2)\, dx \tag{95}$$

upon noting that the cosine argument is always within the region $[0, \pi]$, a region where the cosine decreases. Substitution $u = x^2$ yields

$$\int_0^1 x^2 \cos(\pi x^2)\, dx = 2^{-1} \int_0^1 u^{\frac{1}{2}} \cos(\pi u)\, du \tag{96}$$

$$\leq 2^{-\frac{3}{2}} \int_0^1 \cos(\pi u)\, du = 0 \tag{97}$$

after observing that $u^{\frac{1}{2}} \cos(\pi u) \leq 2^{-\frac{1}{2}} \cos(\pi u)$ on $u \in [0,1]$. The function $\Upsilon(\theta, \omega, \beta)$ is decreasing with respect to $\beta \geq 0$, since (94), (95), and (97) imply that the partial derivative of $\Upsilon(\theta, \omega, \beta)$ with respect to β is negative.

The second preliminary fact that $\Upsilon(\theta, \omega, \beta)$ decreases with respect to ω will be proven similarly by applying the chain rule to compute

$$\frac{\delta \Upsilon(\theta, \omega, \beta)}{\delta \omega} = \int_0^{t_\pi} t \cos(\tilde{\theta} + \omega t + \beta t^2)\, dt. \tag{98}$$

Again let $x = t/t_\pi$, observe that $\beta t_\pi^2 = \pi - \tilde{\theta} - \omega t_\pi$, and apply the same reasoning leading to (95); then

$$\frac{\delta \Upsilon(\theta, \omega, \beta)}{\delta \omega} < t_\pi^2 \int_0^1 x \cos(\pi x^2)\, dx = 0. \tag{99}$$

The partial derivative $\delta \Upsilon(\theta, \omega, \beta)/\delta \omega < 0$ implies the promised result.

The third preliminary fact that $\Upsilon(\omega, \theta, \beta)$ decreases with respect to $\tilde{\theta}$ follows because $\tilde{\theta} = \pi - \omega t_\pi$ implies

$$\Upsilon(\theta, \omega, 0) = \int_0^{t_\pi} \sin(\tilde{\theta} + \omega t)\, dt = \frac{\cos \tilde{\theta} + 1}{\omega}. \tag{100}$$

The fact that $\tilde{\theta} \in [0, \pi)$, a region on which the cosine decreases, clearly demonstrates that $\Upsilon(\theta, \omega, \beta)$ also decreases.

Now with the preliminary facts established, consider $\int_a^b \cos(\theta + \omega t + \beta t^2) dt$ and let $\{\eta_i\}_{i=1}^n$ be, in order, the zeros of the integrand on (a, b). In other words, $a < \eta_{i-1} < \eta_i < b$ and, whenever $t \in (a, b)$, $\cos(\theta + \omega t + \beta t^2) = 0$, if and only if $t = \eta_i$ for some i (if there are no zeros then set $\eta_1 = b$). Decompose the integral into subintegrals between the zeros and get

$$\left| \int_a^b \cos(\theta + \omega t + \beta t^2)\, dt \right| = \left| \sum_{i=0}^{n} (-1)^i e_i \right| \tag{101}$$

where

$$e_i \begin{cases} = \Upsilon\left(\theta - \frac{\pi}{2}, \omega + 2\beta a, \beta\right) & \text{for } i = 0 \\ = \Upsilon\left(0, \omega + 2\beta\eta_i, \beta\right) & \text{for } 0 < i < n \\ \leq \Upsilon\left(0, \omega + 2\beta\eta_n, \beta\right) & \text{for } i = n. \end{cases} \tag{102}$$

Since the e_is are an alternating sequence of elements whose magnitude, after the first element, decreases,

$$\left| \int_a^b \cos(\theta + \omega t + \beta t^2)\, dt \right| \leq \max(e_0, e_1). \tag{103}$$

Use the fact that $\Upsilon(\theta, \omega, \beta)$ decreases with respect to β to maximize e_0, e_1 by putting $\beta = 0$. Next, maximize with respect to the other arguments to show

$$\max(e_0, e_1) \leq \Upsilon(0, \omega + 2\beta a, 0) = \frac{2}{\omega + 2\beta a}. \tag{104}$$

The conclusion of the lemma now follows from (104) and (103).

Definition 1 *Given the partition $\mathcal{P} = [a = t_0 < t_1 \cdots t_{n-1}, t_n = b]$, the positive variation of $x(t)$ on $[a, b]$ is*

$$P_x = \sup_{\mathcal{P}} \sum_{i=1}^{n} [x(t_i) - x(t_{i-1})]^+ + x(a)^+ + x(b)^+ \tag{105}$$

where r^+ has the value r, if $r > 0$, and the value zero, otherwise.

Definition 2 *Given the partition $\mathcal{P} = [a = t_0 < t_1 \cdots t_{n-1}, t_n = b]$, the negative variation of $x(t)$ on $[a, b]$ is*

$$N_x = \inf_{\mathcal{P}} \sum_{i=1}^{n} [x(t_i) - x(t_{i-1})]^- + x(a)^- + x(b)^- \tag{106}$$

where r^- has the value r, if $r < 0$, and the value zero, otherwise.

A function is said to be of bounded variation if both its positive and negative variations are finite.

Lemma 2 *Under the restrictions that $b > a$, $\omega > 0$, $\omega + 2\beta a > 0$, and that $x(t)$ and $y(t)$ are piecewise continuous and of bounded variation on $[a, b]$,*

$$\int_a^b \cos(\theta + \omega t + \beta t^2)x(t)y(t)\,dt \leq \frac{2P_x P_y}{\omega + 2\beta a} \tag{107}$$

where P_x and P_y are the positive variations of $x(t)$ and $y(t)$.

Since the function $x(t)$ is of bounded variation, it is integrable implying that, for arbitrary $\epsilon > 0$, there exists a step function $x_s(t) = \sum_{i=1}^{n} x(t_{i-1})I_{[t_{i-1},t_i]}$ with corresponding partition $[a = t_0 < t_1 \cdots t_{n-1}, t_n = b]$ such that

$$\int_a^b |x(t) - x_s(t)|\,dt < \epsilon. \tag{108}$$

The step function represented above is the sum of nonoverlapping steps. We want to reconstruct it as the sum of overlapping steps with the property that the accumulated absolute amplitudes of the steps are minimal. We do this in an iterated fashion by ordering the step amplitudes $\rho_0 = x(t_{i_0}) \leq \cdots p_{j-1} = x(t_{i_{j-1}})$, $p_j = 0$, $p_{j+1} = x(t_{i_{j+1}}) \cdots \leq \rho_n = x(t_{i_n})$ with the zero amplitude included and defining the increments $l_j = [\rho_{j-1}, \rho_j]$. Starting with the kth step, an increment l_j is considered "open" if $l_j \in [0, \sum_{i=0}^{k} x(t_i)]$ and "closed" otherwise. Whenever an increment l_j transitions from open to closed, define a step of amplitude $r_{k,j} = \mathcal{L}(l_j)$ and of duration $d_{k,j}$ ranging from t_k to the time when the increment was last opened. Proceeding in this manner, the step function now has the form

$$x_s(t) = \sum_{j=0}^{n}\sum_{k=0}^{n} r_{k,j}I_{[t_k, t_k - d_{k,j}]} \tag{109}$$

upon setting $r_{k,j} = 0$ for previously undefined values.

At each stage in the iteration, notice that the sum of the lengths of increments either opened or closed is equal to the variation of the step function at that point, implying that $\sum_{j=0}^{n} r_{k,j} = x(t_j) - x(t_{j-1})$. Notice also that an increment opened by an increase/decrease in the step function can be closed only by a future opposite decrease/increase, meaning every step is uniquely associated with a point of increase. These facts mean that

$$\sum_{j=0}^{n}\sum_{k=0}^{n} r_{k,j} = \sum_{i=1}^{n}[x(t_i) - x(t_{i-1})]^+ + [x(t_0)]^+ \tag{110}$$

$$\leq P_x \tag{111}$$

where the last relation follows from the definition of positive variation. Properly define c_l and τ_l in terms of $r_{k,j}$, t_k, and $d_{k,j}$ to write

$$x_s(t) = \sum_{l=1}^{m} c_l I_{[\tau_{l-1},\tau_l]} \tag{112}$$

with $\sum_{l=1}^{m} c_l \leq P_x$ and $\int_a^b |x(t) - x_s(t)|dt < \epsilon$. A similar step function exists for $y(t)$, namely,

$$y_s(t) = \sum_{l=1}^{n} b_l I_{[u_{l-1},u_l]} \tag{113}$$

with $\sum_{l=1}^{n} b_l \leq P_y$ and $\int_a^b |y(t) - y_s(t)|dt < \epsilon$.

With these two step functions in hand, compute

$$\int_a^b \sin(\theta + \omega t + \beta t^2)x(t)y(t)\,dt = \int_a^b \sin(\theta + \omega t + \beta t^2)x_s(t)y_s(t)\,dt + e(t) \tag{114}$$

where $|e(t)| \leq \epsilon(M_{|x|} + M_{|y|}) + \epsilon^2$, $M_{|x|} = \sup_t |x(t)| < \infty$, and $M_{|y|} = \sup_t |y(t)| < \infty$. Putting (112) and (113) into (114) yields

$$\sum_{k=1}^{m}\sum_{l=1}^{n} b_k c_l \int_a^b \sin(\theta + \omega t + \beta t^2) I_{[\tau_{l-1},\tau_l]\cap[u_{k-1},u_k]}\,dt. \tag{115}$$

Applying Lemma 1 and maximizing the bound by replacing the starting time for each step with the worst case a forms

$$\int_a^b \cos(\theta + \omega t + \beta t^2)x(t)y(t)\,dt \leq \frac{2P_xP_y}{\omega + 2\beta a} - e(t) \tag{116}$$

after noting that $\sum_{l=1}^{m} c_l \leq P_x$ and $\sum_{k=1}^{m} b_k \leq P_y$. Let $\epsilon \to 0$, then $|e(t)| \to 0$ and the lemma is proved.

APPENDIX C

Moments between Squares of Correlated Gaussian Random Variables with Random Phase Component

We have in this section two random variables

$$P = \alpha\cos\theta + \beta\sin\theta + \nu \tag{117}$$

$$Q = \gamma\cos\theta + \delta\sin\theta + \eta \tag{118}$$

where the random variable θ is uniformly distributed on the on $[0, 2\pi]$ and the Gaussian random variables ν and η are zero-mean with covariances σ_ν^2, σ_η^2, and $\sigma_{\nu\eta}^2$. We want to compute the mean and variance of P^2, the mean and variance of P^2, and the covariance between P^2 and Q^2.

Our calculations will be assisted by a formula of the general fourth moment between the Gaussian random variables x_0, x_1, x_2, and x_3 with means $m_i = \mathcal{E}(x_i)$ and covariances $\sigma_{ij}^2 = \mathcal{E}[(x_i - m_i)(x_j - m_j)]$. The formula is

$$\begin{aligned}\mathcal{E}(x_0 x_1 x_2 x_3) &= \sigma_{01}^2\sigma_{23}^2 + \sigma_{02}^2\sigma_{13}^2 + \sigma_{03}^2\sigma_{12}^2 + \sigma_{01}^2 m_2 m_3 + \sigma_{02}^2 m_1 m_3 \\ &+ \sigma_{03}^2 m_1 m_2 + \sigma_{12}^2 m_0 m_3 + \sigma_{13}^2 m_0 m_2 + \sigma_{23}^2 m_0 m_1 \\ &+ m_0 m_1 m_2 m_3. \end{aligned} \tag{119}$$

We will now compute the mean of P^2 and Q^2. Equation (117) implies

$$\mathcal{E}[P^2/\theta] = \alpha^2\cos^2\theta + \beta^2\sin^2\theta + 2\alpha\beta\cos\theta\sin\theta + \sigma_\nu^2 \tag{120}$$

which, upon averaging over θ, becomes

$$\mathcal{E}[P^2] = \frac{\alpha^2}{2} + \frac{\beta^2}{2} + \sigma_\nu^2. \tag{121}$$

Similarly,

$$\mathcal{E}[Q^2] = \frac{\gamma^2}{2} + \frac{\delta^2}{2} + \sigma_\eta^2. \tag{122}$$

Onward to the covariances. Equations (117), (118), and (119) imply that

$$\begin{aligned}\mathcal{E}[P^2Q^2/\theta] &= \sigma_\nu^2\sigma_\eta^2 + 2\sigma_{\nu\eta}^4 + \sigma_\nu^2(\gamma\cos\theta + \delta\sin\theta)^2 \\ &+ 4\sigma_{\nu\eta}^2(\alpha\cos\theta + \beta\sin\theta)(\gamma\cos\theta + \delta\sin\theta) + \sigma_\eta^2(\alpha\cos\theta + \beta\sin\theta)^2 \\ &+ (\alpha\cos\theta + \beta\sin\theta)^2(\gamma\cos\theta + \delta\sin\theta)^2 \end{aligned} \tag{123}$$

which, upon averaging over θ, becomes

$$\begin{aligned}\mathcal{E}[P^2Q^2] &= \sigma_\nu^2\sigma_\eta^2 + 2\sigma_{\nu\eta}^4 + \frac{\sigma_\nu^2}{2}(\gamma^2 + \delta^2) + \frac{\sigma_\eta^2}{2}(\alpha^2 + \beta^2) + 2\sigma_{\nu\eta}^2(\alpha\gamma + \beta\delta) \\ &+ \frac{3}{8}(\alpha^2\gamma^2 + \beta^2\delta^2) + \frac{1}{8}(\gamma^2\beta^2 + 4\alpha\beta\gamma\delta + \alpha^2\delta^2). \end{aligned} \tag{124}$$

With (121), (122), and (124) we conclude that

$$\mathrm{cov}[P^2, Q^2] = 2\sigma_{\nu\eta}^4 + 2\sigma_{\nu\eta}^2(\alpha\gamma + \beta\delta) + \frac{1}{8}(\alpha^2\gamma^2 + \beta^2\delta^2 - \gamma^2\beta^2 - \alpha^2\delta^2) + \frac{1}{2}\alpha\beta\gamma\delta \tag{125}$$

which specializes to

$$\mathrm{var}[P^2] = 2\sigma_\nu^4 + 2\sigma_\nu^2(\alpha^2 + \beta^2) + \frac{1}{8}(\alpha^4 + \beta^4) + \frac{1}{4}\alpha^2\beta^2 \tag{126}$$

$$\mathrm{var}[Q^2] = 2\sigma_\eta^4 + 2\sigma_\eta^2(\gamma^2 + \delta^2) + \frac{1}{8}(\gamma^4 + \delta^4) + \frac{1}{4}\gamma^2\delta^2. \tag{127}$$

APPENDIX D

Derivation of Upper and Lower Bounding Distributions for the Sum of Squares of Correlated Gaussian Random Variables with Random Phase Component

Theorem 1 *Define the n-dimensional vector* $\boldsymbol{P}^T \triangleq [p_1, \cdots, p_n]$ *to have components*

$$p_i \triangleq a_i \cos\theta + b_i \sin\theta + w_i, \quad 1 \le i \le n \tag{128}$$

where each a_i *and* b_i *is a constant,* θ *is a uniformly distributed random variable on* $[0, 2\pi]$*, and* $\{w_i\}_{i=1}^n$ *is a sequence of zero-mean Gaussian random variables with an invertible covariance matrix* $\boldsymbol{\Sigma}$*. Then, with* $\boldsymbol{P}$ *defined as,*

$$1 - Q_{\frac{n}{2}}\left[\sqrt{e_{\max}}, \sqrt{\frac{k}{\lambda_{\max}}}\right] \le Pr\left[\boldsymbol{P}^T\boldsymbol{P} \le k\right] \le 1 - Q_{\frac{n}{2}}\left[\sqrt{e_{\min}}, \sqrt{\frac{k}{\lambda_{\min}}}\right] \tag{129}$$

where $\lambda_{\max}$, $\lambda_{\min}$ *are respectively the maximum and minimum eigenvalues of* $\boldsymbol{\Sigma}$ *and where* $e_{\max}$, $e_{\min}$ *are respectively the maximum and minimum eigenvalues of the matrix*

$$\boldsymbol{B} \triangleq \boldsymbol{A}^T\boldsymbol{\Sigma}\boldsymbol{A} \tag{130}$$

with

$$\boldsymbol{A} \triangleq \begin{bmatrix} a_1 & b_1 \\ \vdots & \vdots \\ a_n & b_n \end{bmatrix} \tag{131}$$

and, finally, where Q_m *is the generalized Marcum Q-function defined as*

$$Q_m(\alpha, \beta) \triangleq \int_\beta^\infty x\left(\frac{x}{\alpha}\right)^{m-1} e^{-\frac{1}{2}(x^2+\alpha^2)} I_{m-1}(\alpha x)\, dx. \tag{132}$$

Proof: The proof consists of three parts. In the first part, the conditional probability $\Pr[\boldsymbol{P}^T\boldsymbol{P} \le k/\theta]$ is expressed as an integral of a multidimensional Gaussian density over a spheroid centered at the origin. Upon transformation with a decorrelating matrix, the region of integration becomes ellipsoidal and the Gaussian density becomes independent, with each of its marginal densities having unity variance. Then through eigenvalue analysis, the ellipsoidal region of integration is inscribed and circumscribed with spheroids yielding corresponding bounds on the integral. The second part of the proof shows that the integral of an independent Gaussian distribution over an arbitrary spheroid depends only on the magnitude of the mean vector and decreases with respect to it. This fact enables further bounding in the third part after computing the minimum and maximum of the mean as a function of θ. An aftereffect is the removal of θ dependence in the bounds, thus allowing their direct application to the unconditional probability $\Pr[\boldsymbol{P}^T\boldsymbol{P} \le k]$. Next the bounds, which are still expressed as integrals, are evaluated in closed form via the generalized Marcum Q-function.

Part i: By applying the expression for a multivariate Gaussian density, the conditional probability

$$\Pr[\boldsymbol{P}^T\boldsymbol{P} \le k/\theta] = \frac{1}{2\pi\,|\boldsymbol{\Sigma}|^{\frac{1}{2}}} \int_{\left[\boldsymbol{P}^T\boldsymbol{P} \le k\right]} e^{-\frac{1}{2}[\boldsymbol{P}-\boldsymbol{AC}]^T\boldsymbol{\Sigma}^{-1}[\boldsymbol{P}-\boldsymbol{AC}]}\,d\boldsymbol{P} \tag{133}$$

where

$$\boldsymbol{C} = \begin{bmatrix} \cos\theta \\ \sin\theta \end{bmatrix}. \tag{134}$$

The matrix $\boldsymbol{\Sigma}^{-\frac{1}{2}}$ with the property $\boldsymbol{\Sigma}^{-\frac{T}{2}}\boldsymbol{\Sigma}^{-\frac{1}{2}} = \boldsymbol{\Sigma}^{-1}$ is guaranteed to exist, since $\boldsymbol{\Sigma}$ is an invertible covariance matrix. Furthermore, for the same reason, there exists an orthogonal matrix $\boldsymbol{T}$, such that $\boldsymbol{\Sigma} = \boldsymbol{T}^T\boldsymbol{\Lambda}\boldsymbol{T}$, where $\boldsymbol{\Lambda}$ is a diagonal matrix of eigenvalues of $\boldsymbol{\Sigma}$. We can now define the transformation $\boldsymbol{X} = \boldsymbol{T}\boldsymbol{\Sigma}^{-\frac{1}{2}}\boldsymbol{P}$, from which follows

$$\Pr[\boldsymbol{P}^T\boldsymbol{P} \le k/\theta] = \frac{1}{2\pi} \int_{\left[\boldsymbol{X}^T\boldsymbol{\Lambda}\boldsymbol{X} \le k\right]} e^{-\frac{1}{2}[\boldsymbol{X}-\boldsymbol{M}_\theta]^T[\boldsymbol{X}-\boldsymbol{M}_\theta]}\,d\boldsymbol{X} \tag{135}$$

where

$$\boldsymbol{M}_\theta = \boldsymbol{T}\boldsymbol{\Sigma}^{-\frac{1}{2}}\boldsymbol{AC}. \tag{136}$$

Now, since $\boldsymbol{\Sigma}$ is an invertible covariance matrix, each entry of $\boldsymbol{\Lambda}$ (i.e. eigenvalues of $\boldsymbol{\Sigma}$) is positive.

Hence

$$\left[\lambda_{\max} X^T X \le k\right] \subset \left[X^T \Lambda X \le k\right] \subset \left[\lambda_{\min} X^T X \le k\right] \tag{137}$$

from which

$$\Pr[P^T P \le k/\theta] \ge \frac{1}{2\pi} \int_{\left[X^T X \le k/\lambda_{\max}\right]} e^{-\frac{1}{2}[X-M_\theta]^T[X-M_\theta]}\, dX \tag{138}$$

and

$$\Pr[P^T P \le k/\theta] \le \frac{1}{2\pi} \int_{\left[X^T X \le k/\lambda_{\min}\right]} e^{-\frac{1}{2}[X-M_\theta]^T[X-M_\theta]}\, dX. \tag{139}$$

Part ii: We aim to show that, for a given r,

$$R \triangleq \frac{1}{2\pi} \int_{\left[X^T X \le r\right]} e^{-\frac{1}{2}[X-M]^T[X-M]}\, dX \tag{140}$$

depends only on the magnitude of M and decreases as $|M|$ gets larger.

There exists an orthogonal matrix U, such that $UM = [|M|, 0, \cdots, 0]^T$. The matrix U is simply a change of orthonormal basis to one that includes $M/|M|$ as its first member. Now $Y = UX$ transforms (140) to

$$R = \frac{1}{2\pi} \int_{\left[Y^T Y \le r\right]} e^{-\frac{1}{2}(y_1 - |M|)^2 - \frac{1}{2}\sum_{i=2}^{n} y_i^2}\, dY. \tag{141}$$

As promised for a given r, (141) depends only on the magnitude of M, hence the notation $R(|M|)$.

We now show that $R(|M|)$ decreases with respect to the magnitude of M by showing that, for any positive increment $\Delta|M|$, the corresponding difference $\Delta R(|M|) \triangleq R(|M| + \Delta|M|) - R(|M|)$ is negative.

Make the respective substitutions $z_1 = y_1 - |M|$, $z_i = y_i$, for $2 \le i \le n$, to $R(|M|)$ and $z_1 = y_1 - |M| - \Delta|M|$, $z_i = y_i$, for $2 \le i \le n$, to $R(|M| + \Delta|M|)$. Then

$$\Delta R(|M|) = \frac{1}{2\pi} \int_G e^{-\frac{1}{2}Z^T Z}\, dZ - \frac{1}{2\pi} \int_H e^{-\frac{1}{2}Z^T Z}\, dZ \tag{142}$$

where the sets G and H are

$$G = \left[Z : (z_1 + |M| + \Delta|M|)^2 + \sum_{i=2}^{n} z_i^2 \le r\right] \tag{143}$$

$$H = \left[Z : (z_1 + |M|)^2 + \sum_{i=2}^{n} z_i^2 \le r\right]. \tag{144}$$

Cancel out the common points of G and H then

$$\Delta R(|M|) = \frac{1}{2\pi}\int_{G\sim H} e^{-\frac{1}{2}Z^T Z}\, dZ - \frac{1}{2\pi}\int_{H\sim G} e^{-\frac{1}{2}Z^T Z}\, dZ. \tag{145}$$

Let $v_1 = -z_1 - 2|M| - \Delta|M|$, $v_i = z_i$, for $2 \leq i \leq n$, in the second integral above; then $H \sim G$ is mapped to $G \sim H$ and the integrals can be combined to yield

$$\Delta R(|M|) = \frac{1}{2\pi}\int_{G\sim H} e^{-\frac{1}{2}\sum_{i=1}^{n} z_i^2}\left[1 - e^{-\frac{1}{2}(2|M|+\Delta|M|)^2 - z_1(2|M|+\Delta|M|)}\right] dZ. \tag{146}$$

The coordinate z_1 is in $G \sim H$, if and only if

$$(z_1 + |M|)^2 + 2\Delta|M|(z_1 + |M|) + (\Delta|M|)^2 + \sum_{i=2}^{n} z_i \leq r \tag{147}$$

and

$$(z_1 + |M|)^2 + \sum_{i=2}^{n} z_i > r. \tag{148}$$

Upon subtracting both relations, z_1 must satisfy

$$z_1 < -|M| - \frac{\Delta|M|}{2}. \tag{149}$$

Using this relationship in (146) implies that $\Delta R(|M|) < 0$, meaning that $R(|M|)$ decreases with increasing magnitude of M.

Part iii: Further bound (138) and (139) by respectively maximizing and minimizing magnitude of the mean over the random phase θ. From (136), the magnitude of the mean is

$$|\boldsymbol{M}_\theta|^2 = \boldsymbol{M}_\theta{}^T \boldsymbol{M}_\theta = \boldsymbol{C}^T \boldsymbol{A}^T \boldsymbol{\Sigma}^{-1} \boldsymbol{A}\boldsymbol{C} \tag{150}$$

following from the fact that $\boldsymbol{T}$, being orthogonal, satisfies $\boldsymbol{T}^T\boldsymbol{T} = \boldsymbol{I}$. The matrix $\boldsymbol{A}^T\boldsymbol{\Sigma}^{-1}\boldsymbol{A}$, being symmetric, ensures that it can be diagonalized making

$$|\boldsymbol{M}_\theta|^2 = [\cos\theta, \sin\theta]\boldsymbol{U}^T \begin{bmatrix} e_{\max} & 0 \\ 0 & e_{\min} \end{bmatrix} \boldsymbol{U} \begin{bmatrix} \cos\theta \\ \sin\theta \end{bmatrix} \tag{151}$$

where $\boldsymbol{U}$ is an orthogonal matrix and $e_{\max}$ and $e_{\min}$ are the eigenvalues of $\boldsymbol{A}^T\boldsymbol{\Sigma}^{-1}\boldsymbol{A}$. Since $\boldsymbol{U}$ is orthogonal, it rotates the plane by some angle ϕ. This means that

$$\boldsymbol{U}\begin{bmatrix} \cos\theta \\ \sin\theta \end{bmatrix} = \begin{bmatrix} \cos(\theta - \phi) \\ \sin(\theta - \phi) \end{bmatrix} \tag{152}$$

and hence that

$$|M_\theta|^2 = e_{\max}\cos^2(\theta-\phi) + e_{\min}\sin^2(\theta-\phi). \tag{153}$$

The eigenvalues $e_{\max}$ and $e_{\min}$ are nonnegative since $A^T\Sigma^{-1}A$ has a square root, namely, $\Sigma^{-\frac{1}{2}}A$. This fact, along with (153), implies

$$\sqrt{e_{\min}} \le |M_\theta| \le \sqrt{e_{\max}}. \tag{154}$$

Use (154) and (141) to deduce from (139) and (138) the bounds

$$\Pr[P^TP \le k] \ \ge \ \frac{1}{2\pi}\int_{\left[Y^TY \le k/\lambda_{\max}\right]} e^{-\frac{1}{2}\sum_{i=2}^{n} y_i^2 - \frac{1}{2}(y_1-\sqrt{e_{\max}})^2}\, dY \tag{155}$$

$$\Pr[P^TP \le k] \ \le \ \frac{1}{2\pi}\int_{\left[Y^TY \le k/\lambda_{\min}\right]} e^{-\frac{1}{2}\sum_{i=2}^{n} y_i^2 - \frac{1}{2}(y_1-\sqrt{e_{\min}})^2}\, dY. \tag{156}$$

The integrals in the above bounds are simplified by showing that they are the distribution functions, evaluated respectively at $k/\lambda_{\max}$ and $k/\lambda_{\min}$ of the sum of n non-central χ^2 random variables with noncentrality $e_{\max}$, $e_{\min}$. An explicit expression for this distribution is given in [2] and leads to the conclusion of the theorem:

$$1 - Q_{\frac{n}{2}}\left[\sqrt{e_{\max}}, \sqrt{\frac{k}{\lambda_{\max}}}\right] \le \Pr\left[P^TP \le k\right] \le 1 - Q_{\frac{n}{2}}\left[\sqrt{e_{\min}}, \sqrt{\frac{k}{\lambda_{\min}}}\right]. \tag{157}$$

References

[1] M.K. Simon, J.K. Omura, R.A. Scholtz, and B.K. Levitt, *Spread Spectrum Communications*, vol III, Computer Sciences Press, Rockville, Md., 1985.

[2] D. Torrieri, *Principles of Secure Communication Systems*. Artech House, Dedham, Mass., 1985.

[3] A. Polydoros, J.K. Holmes and K.T. Woo, "Advanced LPI Intercept Detector Research", Technical Report No. R8511-3, Axiomatix, Los Angeles, Calif., November 13, 1985.

[4] W.E. Snelling and E.A. Geraniotis, "Sequential Detection of Unknown, Fast Frequency-Hopped Waveforms", *IEEE J. Select. Areas Commun.*, vol. 7, no. 4, pp. 602–617, May 1989.

[5] K.D. Breuer, J.J Whelehan, and K. Ross, "Compressive Receivers Applied to ESM System Design", *MSN Microwave Syst. News & Commun. Techno.*, vol. 16, no. 11, pp. 66–68, 70, 72, 74–75, Oct. 1986.

[6] B.K. Harms and D.R. Hummels, "Calculation of Detection Probability for Frequency Compressive Receivers", *IEEE Trans. Aerospace and Electronic Systems*, vol. AES-21, pp. 106–116, January 1985.

[7] K.H. Li and L.B. Milstein, "On the Use of a Compressive Receiver for Signal Detection", to be published in *IEEE Trans. Commun.*

[8] H.L. van Trees, *Detection, Estimation, and Modulation Theory, Part I*, Wiley, New York, 1968.

[9] A. Papoulis, *Probability, Random Variables, and Stochastic Processes*, Second Edition, McGraw-Hill, New York, 1984.

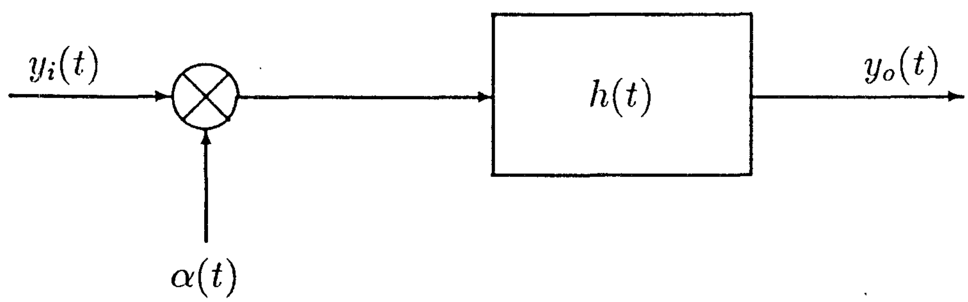

Figure 1: Block Diagram of Compressive Receiver Model

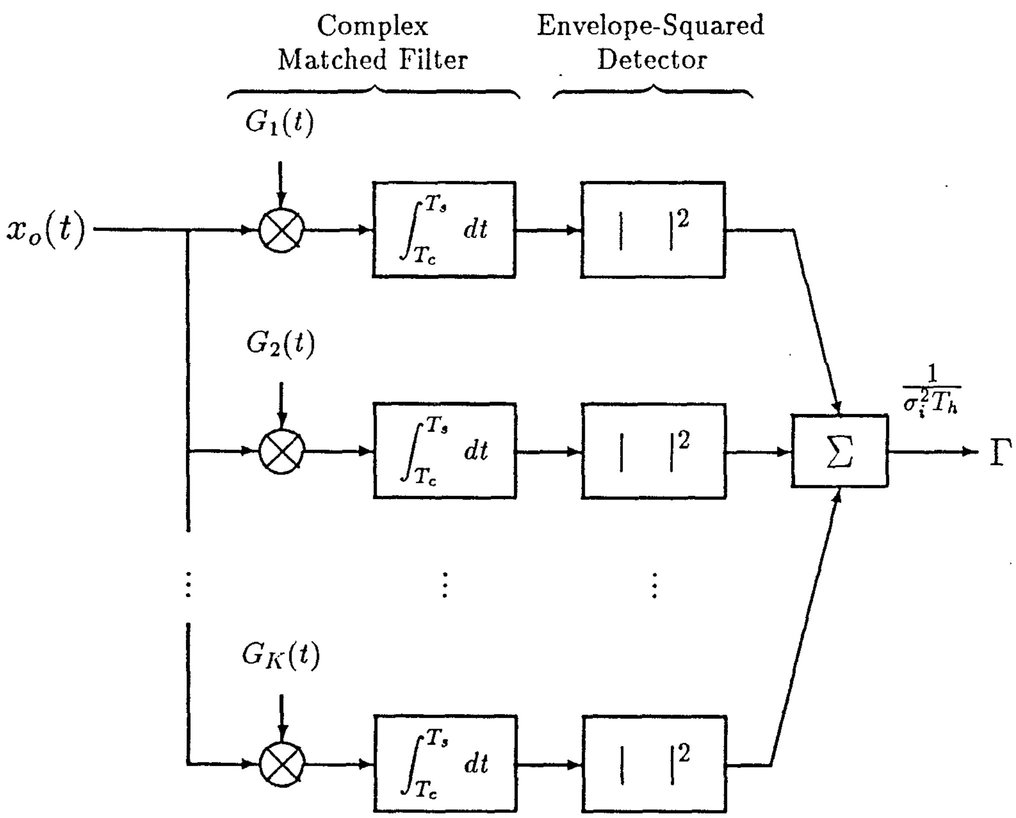

Figure 2: Locally Optimal Single-Epoch Detector

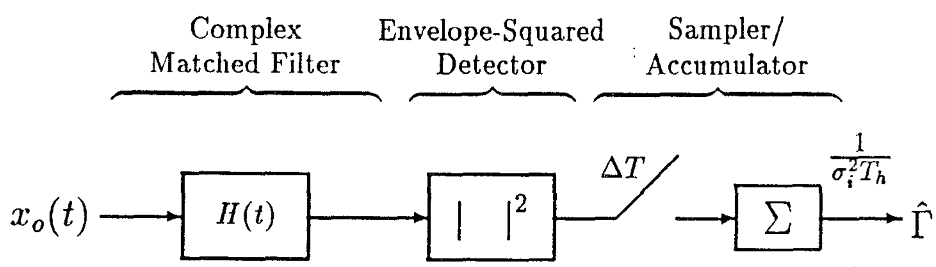

Figure 3: Simple-Filter Detector

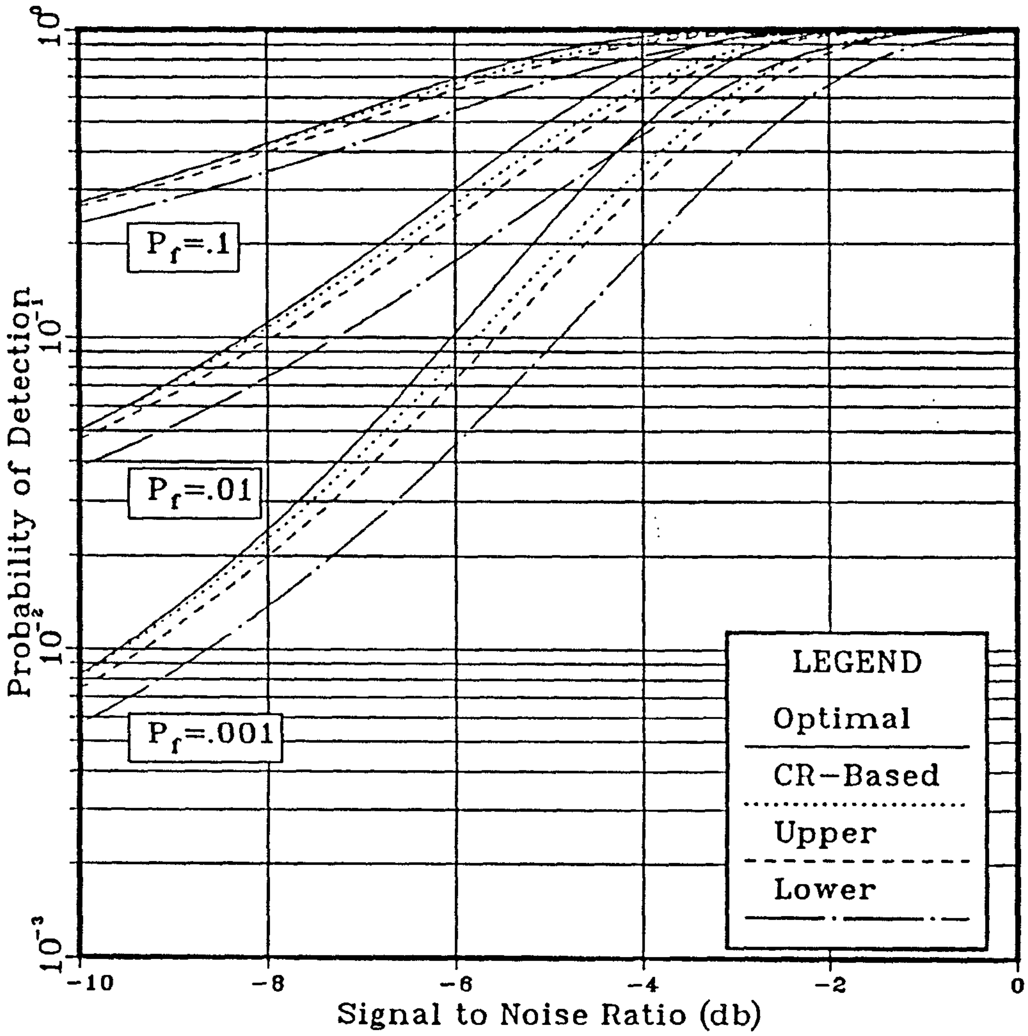

Figure 4: Performance of Locally Optimal Detector Based on Compressive Receiver Observations versus Optimal, Filter Bank Detector Based on Direct Observations

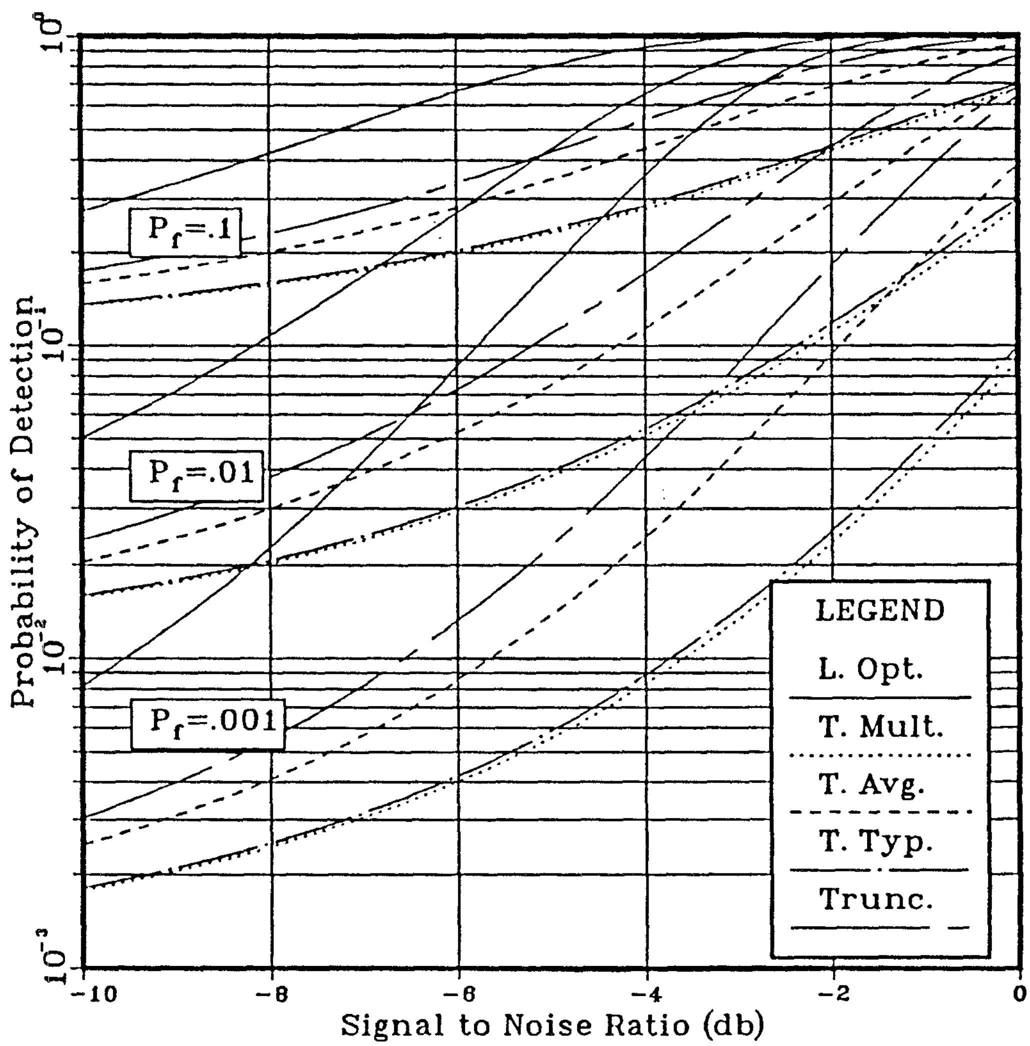

Figure 5: Performance of Locally Optimal Detector Compared with Time-Multiplexed Detector

Table 1: Coefficients of (83)

j	θ_j	ω_j	β_j
1	$2\omega_0 t - 2\beta t^2 - \frac{\beta}{2}d^2 + \beta d u_1$	$2\beta t$	0
2	$-2\omega_0 t + 2\beta t^2 + \frac{\beta}{2}d^2 - \beta d u_1 + \beta u_1^2$	$2\omega_0 - 2\beta t$	β
3	$-(\omega_0 - 2\beta t)(u_1 - d) + \frac{\beta}{2}u_1^2$	$\omega_0 + \beta d - \beta u_1$	$\frac{\beta}{2}$
4	$-2\omega_0 t + 2\beta t^2 + \frac{\beta}{2}d^2 - (\omega_0 + \beta d)u_1 + \frac{\beta}{2}u_1^2$	$\omega_0 - 2\beta t - \beta u_1$	$\frac{\beta}{2}$
5	$(\omega_0 - 2\beta t)(u_1 - d) + \frac{\beta}{2}u_1^2$	$\omega_0 - \beta d + \beta u_1$	$\frac{\beta}{2}$
6	$-2\omega_0 t + 2\beta t^2 + \frac{\beta}{2}d^2 + (\omega_0 - \beta d)u_1 + \frac{\beta}{2}u_1^2$	$\omega_0 - 2\beta t + \beta u_1$	$\frac{\beta}{2}$
7	$\omega_0 d + 2\beta t(u_1 - d)$	βd	0
8	$(\omega_0 - 2\beta t)d + (-2\omega_0 + 2\beta t)u_1$	$\beta d - 2\beta u_1$	0